Mechanism Dictates Mechanics: A Molecular Substituent Effect in the Macroscopic Fracture of a Covalent Polymer Network

Shu Wang †,‡ , Haley K. Beech $^{\dagger,\parallel}$, Brandon H. Bowser †,‡ , Tatiana B. Kouznetsova †,‡ , Bradley D. Olsen $^{*,\dagger,\parallel}$, Michael Rubinstein $^{*,\dagger,\ddagger,\$}$ and Stephen L. Craig *,†,‡

†NSF Center for the Chemistry of Molecularly Optimized Networks; ‡Department of Chemistry, [§]Departments of Physics, Mechanical Engineering, and Biomedical Engineering, Duke University, Durham, North Carolina 27708, United States; [∥]Department of Chemical Engineering, Massachusetts Institute of Technology, Cambridge, Massachusetts 02139, United States;

ABSTRACT: The fracture of rubbery polymer networks involves a series of molecular events, beginning with conformational changes along the polymer backbone and culminating with a chain scission reaction. Here, we report covalent polymer gels in which the macroscopic fracture "reaction" is controlled by mechanophores embedded within mechanically active network strands. We synthesized poly(ethylene glycol) (PEG) gels through the end-linking of azide-terminated tetra-arm PEG (M_n = 5 kDa) with bis-alkyne linkers. Networks were formed under identical conditions, except that the bis-alkyne was varied to include either a *cis*-diaryl (1) or *cis*-dialkyl (2) linked cyclobutane mechanophore that acts as a mechanochemical "weak link" through a force-coupled cycloreversion. A control network featuring a bis-alkyne without cyclobutane (3) was also synthesized. The networks show the same linear elasticity (G' = 23~24 kPa, 0.1 – 100 Hz) and equilibrium mass swelling ratios (Q = 10~11 in tetrahydrofuran), but they exhibit tearing energies that span a factor of 8 (3.4 J·m⁻², 10.6 J·m⁻², and 27.1 J·m⁻² for networks with 1, 2, and 3, respectively). The difference in fracture energy is well aligned with the force-coupled scission kinetics of the mechanophores observed in single-molecule force spectroscopy experiments, implicating local resonance stabilization of a diradical transition state in the cycloreversion of 1 as a key determinant of the relative ease with which its network is torn. The connection between macroscopic fracture and small molecule reaction mechanism suggests opportunities for molecular understanding and optimization of polymer network behavior.

The fracture of rubbery covalent polymer networks limits the lifetime and utility of biomedical implants, consumer products,² and soft devices for emerging applications.³ Network fracture is most commonly perceived macroscopically, for example by how difficult it is to tear a contact lens relative to a piece of gelatin or an automobile tire. Concepts of very specific chemical reactivity are rarely invoked. The macroscopic event, however, comprises of a series of molecular events, including low energy conformational changes and higher energy bond stretching, that culminate in a covalent chemical reaction: the scission of network strands that bridge the growing crack plane. Thus, it should be possible to connect behaviors on two very different length scales: the local molecular structure (e.g., substituent effects) that dictate chemical reactivity, and the macroscopic tearing of bulk material. Here, we report covalent polymer gels in which the reactivity of a single functional group within a network strand dictates the fracture energy.

Our approach, described in Figure 1a, is to embed a mechanophore $^{4.5}$ into each elastically active strand of a polymer network, systematically varying the mechanochemical reactivity in the otherwise identical networks. We chose cyclobutane-based mechanophores $^{6-8}$ whose reactivity through scissile cycloreversion differs as a result of the substituent (aryl vs. methylene, dark vs. light blue in Figure 1b) on the cyclobutane ring. The mechanochemical reactivity of the diaryl cyclobutane was previously characterized by Weng and co-workers using single-molecule force spectroscopy (SMFS), and a force of 1.0 ± 0.1 nN is required to reduce the half-life for cycloreversion to $\sim\!40$ ms. 9 We expected that converting the aryl substituents of I to

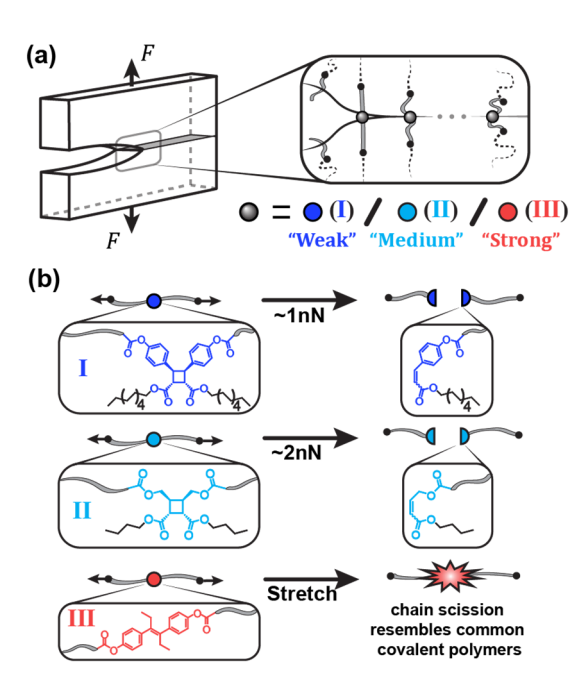


Figure 1. (a) Schematic illustration of embedding mechanochemically (I) "weak" and (II) "medium" mechanophores, and a (III) "strong" control structure into the otherwise identical networks. (b) Structures, force-coupled reactivities and the reaction mechanisms of I and II.

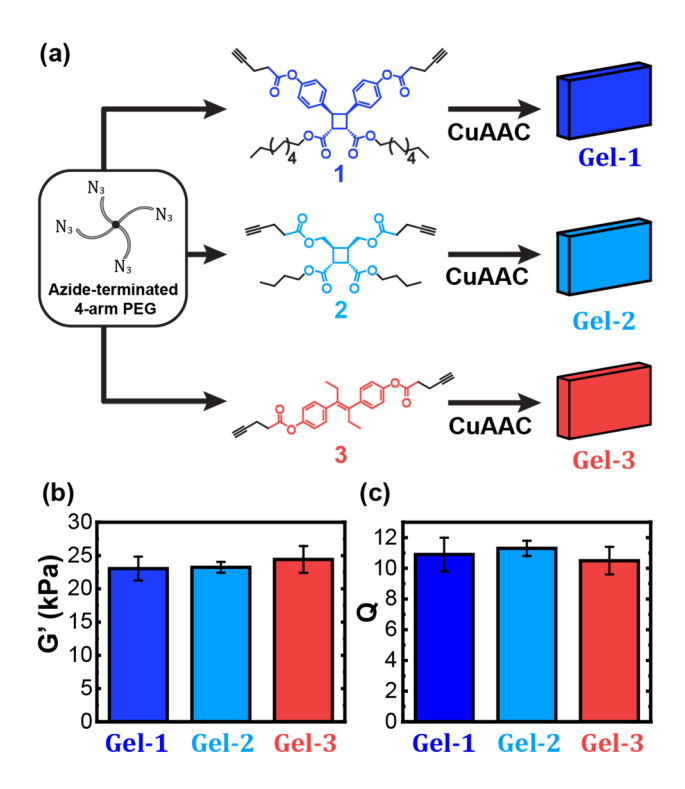


Figure 2. (a) Schematic illustration of gel preparation; all gels were prepared at the same condition. (b) Frequency sweeps of gels performed in the as-prepared state. (c) Equilibrium swelling ratios in THF.

methylenes in II would increase the force necessary for cycloreversion, and SMFS studies using methods reported previously 10,11 revealed that much larger forces (2.1 \pm 0.1 nN) are required to achieve the same lability (See Supporting Information for PII).

These mechanophores were incorporated into polymer networks as shown in Figure 2. Mechanophores I and II were incorporated into bis-alkyne linkers 1 and 2, respectively (Figure 2a). A bis-alkyne linker (3) without cyclobutane was synthesized as a control. Linkers 1-3 were each then reacted via copper(I)-catalyzed azide-alkyne cycloaddition (CuAAC)^{12,13} with azide-terminated tetra-arm PEG (M_n = 5 kDa), prepared as previously reported^{14,15} to form the corresponding networks Gel-1, Gel-2, and Gel-3. Networks were formed under identical preparation conditions (25 mM PEG, alkyne : azide = 1 : 1, propylene carbonate as solvent). The preparation volume fraction $\phi_0 \approx$ 0.11 was chosen to be just above the overlap volume fraction $\phi^* = 0.097$ and well below the entanglement volume fraction, ^{16,17} so that the load in every elastically active strand must be transmitted through a linker. Further details of the gel preparation can be found in Supporting Information.

We next verified that, aside from the content of the linker segment, **Gels 1-3** have effectively identical network structure. Shear moduli were measured with small amplitude oscillatory shear rheology in the as-prepared state. All three networks exhibit frequency-independent storage moduli G' across frequencies of 0.1-100 s⁻¹, and the average moduli of the networks are indistinguishable within experimental uncertainty across five different characterizations: 23.0 ± 1.8 kPa, 23.2 ± 0.8 kPa, and 24.4 ± 2.0 kPa, respectively (**Figure 2b**). The similar moduli indicate that the CuAAC polymerization is, as expected, similarly efficient across the networks, resulting in an indistinguish-

able number and distribution of elastically active strands. Further confirmation of structural homology comes from removing the propylene carbonate and immersing the formed networks in excess tetrahydrofuran; as with the elastic moduli, the equilibrium mass swelling ratios Q, defined as the mass ratio between the fully swollen and dry states, are statistically equivalent across four independent measurements: 10.9 ± 1.1 , 11.3 ± 0.5 , and 10.5 ± 0.9 , respectively (**Figure 2c**).

We then characterized the impact of the embedded mechanophores on the strength of the network. A first indication of significant effect came from simply handling the materials; we were struck by the obvious differences in their tactile behavior. In particular, the texture of Gel-1 is more fragile to the touch than Gel-2 – to the point that it feels "crumbly" during sample transfer. Care is needed when introducing a notch to Gel-1 with a razor blade for tear testing, as uncontrolled cuts result in the entire piece falling apart. In contrast, Gel-2 is much easier to handle, but it still showed noticeably less resistance than Gel-3 when cut with a punch or a razor blade. The gels have negligible differences in chemical composition and low strain, linear mechanical properties, and this qualitative observation suggested that there must be differences in mechanical properties that are associated with the behavior of the linkers at higher strains.

The stress-strain curves of unnotched and notched samples under uniaxial tension are shown in **Figure 3a,b**. As with the oscillatory rheology, the stress-strain behavior of the unnotched samples is identical up to the point of fracture, but the critical strain required for fracture (peak stress in the stress-strain curve) goes in the order **Gel-1** < **Gel-2** < **Gel-3**. The difference in strength is better quantified through the tearing energies, Γ , obtained from the strain necessary for the propagation of a crack introduced into notched samples. Unlike the moduli, the tearing energies are significantly different across the gels: $3.4 \pm 1.5 \text{ J} \cdot \text{m}^{-2}$, $10.6 \pm 1.7 \text{ J} \cdot \text{m}^{-2}$, and $27.1 \pm 1.6 \text{ J} \cdot \text{m}^{-2}$ for **Gel-1**, **Gel-2**, and **Gel-3**, respectively (**Figure 3c**).

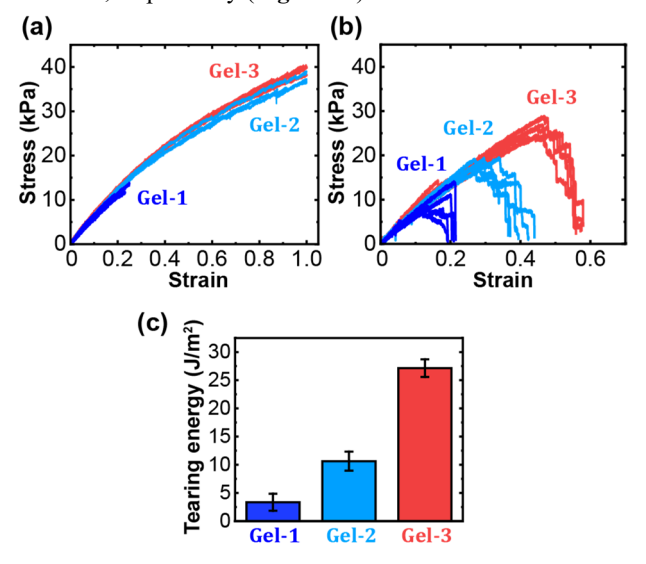


Figure 3. Stress-strain curves for (a) unnotched and (b) notched samples of **Gel 1-3**. (c) Tearing energies of **Gel 1-3**. All measurements were performed at the as-prepared state.

The difference in tearing energies is attributed to the only significant difference in the gels – the single mechanophore present in each linker. In strands made from 1 and 2, the mechanical "weak bond"^{19,20} is the cyclobutane mechanophore, whereas the site of scission in strands incorporating 3 is less clear. We

hypothesize that the likely scission pathway is α -cleavage at the C-C bond next to the 1,4-disubstituted 1,2,3-triazole ring, which has been reported to be a mechanochemically weak site, ²¹ but other possibilities include bonds at highly substituted centers such as the junctions of the 4-arm PEG and the α carbon of isobutyrate ester.

The correlations highlight an important distinction. To date, many molecular interpretations of polymer fracture are based on the well-known Lake-Thomas theory,²² which connects the fracture energy of the polymer network to the energy stored per chain along the elastically active strand when it breaks. Such interpretations of polymer fracture energies default to the thermodynamics of the bond scission reaction (e.g. total bond dissociation energy) as the relevant molecular thermodynamic quantity.^{23,24} The systems employed here reveal limitations of this assumption, as the total BDEs (enthalpy of the cycloreversion reaction) for cyclobutane scission in 1 is exothermic, 9 and so fracture would require no energy. Instead, the relevant molecular parameters are associated with the kinetics of reactivity, as captured in SMFS measurements of force-coupled bond lifetimes for 1 and 2. As noted above, the forces required for lifetimes of tens of ms are roughly 1 nN and 2 nN for 1 and 2, respectively, whereas extrapolating prior calculations by Smalø and Uggerud gives a corresponding value of ~3 nN for triazole α -cleavage in 3.²¹

According to the Lake-Thomas theory, 22 when the number of broken chains is constant, the fracture energy Γ is proportional to the energy stored per strand at rupture, U. Based on recent adjustments 25,26 to the Lake-Thomas theory, the energy U is approximately proportional to the square of the breaking tension of the bridging strands $(U \sim f_{break}^2)$, because the stored elastic energy of the bridging polymer chain is dominated by enthalpic deformation that is assumed to have a spring-like, linear forcedisplacement dependence. A quadratic dependence is expected if the majority of the stored energy is not held within the bridging strands, but in the much softer (lower force constant), but still spring-like, entropic deformations of non-bridging strands connected to the bridging strands in a tree-like structure. Assessing these molecular theories, however, requires knowledge of the actual breaking forces of the strands during crack propagation, which likely differ from those measured by SMFS, because the loading conditions during fracture and SMFS are not identical. Unfortunately, the precise single-chain loading rates at the propagating fracture plane are not known, but we offer a rough estimate based on fracture mechanics, SMFS experiments and mechanical tests, and simulated data.

Based on previously reported treatments of steady-state fracture processes, the relevant strain rates at the process/plastic zone for **Gels 1-3** are estimated to be $\sim 10^2$ s⁻¹.²⁷ The reported stretch stiffness of linear PEG is about 100 nN in the enthalpic deformation regime at which strand scission occurs, 28 and so the operative loading rate (product of strain rate and strand stretch stiffness) per strand is estimated to be on the order of 10⁴ nN/s (see Supporting Information). Using previously reported force dependence⁹ and applying the Bell model for force-dependent bond scission under dynamic loading, the rate constant of I at a loading rate of 10⁴ nN/s is estimated to be about 10⁵ s⁻¹, and the average force at break is about 1.3 nN (see Supporting Information). Estimates of 2.6 nN for II and 3.8 nN for III are obtained using calculations by Boulatov and coworkers9 and Smalø and Uggerud,²¹ respectively (see Supporting Information). Fitting these data to a power law dependence (Figure **S4)**, $\Gamma \sim f_{break}^a$, provides a value of a = 1.9 across the series of gels, in comparison to a = 2 expected from the "coupled spring" models described above. Given the assumptions involved in this treatment, a more complete and quantitative examination of the relationship between macroscopic tearing energy and strand scission force is desirable. In particular, future efforts will benefit from a detailed characterization of: network topology, ^{15,29} the effective strain rate at the crack tip, and the precise rate-force dependence of strand scission for these mechanophores.

Nonetheless, the results suggest a direct connection between macroscopic and molecular behavior. **Gel-1** and **Gel-2** are structurally indistinguishable, with the notable exception of the difference in aryl vs. methylene substituents at a single moiety in the linker connecting tetra-PEG macromers. The total aryl group content of **Gel-1** is 0.55 wt. % and immersed within a majority mobile solvent phase, and yet, as noted above, the two gels are easily distinguished by their feel to human touch. The difference in network properties that is actually being felt by hand, in essence, is the connection between tearing energy and force-coupled reactivities of the embedded mechanophores on each strand.

We note the likely origins of the underlying reactivity differences. Although the cycloreversion mechanism of **II** has not been studied explicitly, it is expected to have a diradicaloid transition state akin to similar cyclobutanes. ^{9,30,31} Relative to **II**, therefore, the lower activation force of **I** can be attributed in large part to the stabilization of the diradical transition state ^{9,31,32} by the aryl substituents, in large part through quantum mechanical effects manifested as resonance stabilization. ³³ Ultimately, the differences in macroscopic behavior that are easily felt by hand originate in these molecular-scale electronic substituent effects.

Additional implications of these results include the opportunity to expand the use of mechanophores as quantitative probes of molecular fracture mechanisms. Mechanochromic and mechanoluminescent mechanophores are providing molecular insights by enabling visualization of the damage zone, 34,35 and scissile mechanophores with known force-coupled reactivity complement those tools by connecting the structural observations to quantitative relationships between macroscopic and molecular mechanical responses. That opportunity motivates further characterizations of the force dependency of mechanochemical reactions^{8,36–41} that are suited to this purpose, noting that historical connections between strand scission and bond dissociation energies are prone to error and become less valid as strands break through reaction mechanisms other than homolytic scission. Together with a better understanding of the relevant loading rate and associated reaction dynamics at the propagating crack tip, such efforts might ultimately lead to quantitative, first-principles prediction of macroscopic fracture behavior as a function of network molecular structure.

ASSOCIATED CONTENT

Supporting Information. Synthetic procedures, gel preparation and characterizations, SMFS details, estimates of strain rates and single-chain loading rates in the process zone, estimates of singe-chain activation forces at the loading rate of 10⁴ nN/s. This material is available free of charge via the Internet at http://pubs.acs.org.

AUTHOR INFORMATION

Corresponding Author

- *Bradley D. Olsen, bdolsen@mit.edu
- *Michael Rubinstein, mr351@duke.edu
- *Stephen L. Craig, stephen.craig@duke.edu

Funding Sources

This work was funded by Duke University and the Center for the Chemistry of Molecularly Optimized Networks (MONET), a National Science Foundation (NSF) Center for Chemical Innovation (CHE-1832256).

Notes

The authors declare no competing financial interest.

ACKNOWLEDGMENT

This work was funded by Duke University and the Center for the Chemistry of Molecularly Optimized Networks (MONET), a National Science Foundation (NSF) Center for Chemical Innovation (CHE-1832256 to S.L.C., M.R., and B.D.O.). B.B. acknowledges a Paul M. Gross Fellowship from Duke University.

REFERENCES

- (1) De Coninck, T.; Huysse, W.; Willemot, L.; Verdonk, R.; Verstraete, K.; Verdonk, P. Two-Year Follow-up Study on Clinical and Radiological Outcomes of Polyurethane Meniscal Scaffolds. *Am. J. Sport. Med.* **2013**, *41*, 64–72.
- (2) Mars, W. V.; Fatemi, A. A Literature Survey on Fatigue Analysis Approaches for Rubber. *Int. J. Fatigue* 2002, 24 (9), 949–961.
- (3) Root, S. E.; Savagatrup, S.; Printz, A. D.; Rodriquez, D.; Lipomi, D. J. Mechanical Properties of Organic Semiconductors for Stretchable, Highly Flexible, and Mechanically Robust Electronics. *Chem. Rev.* 2017, 117 (9), 6467–6499.
- (4) Izak-Nau, E.; Campagna, D.; Baumann, C.; Göstl, R. Polymer Mechanochemistry-Enabled Pericyclic Reactions. *Polym. Chem.* 2020, 11, 2274–2299.
- (5) Ghanem, M. A.; Basu, A.; Behrou, R.; Boechler, N.; Boydston, A. J.; Craig, S. L.; Lin, Y.; Lynde, B. E.; Nelson, A.; Shen, H.; Storti, D. W. The Role of Polymer Mechanochemistry in Responsive Materials and Additive Manufacturing. *Nat. Rev. Mater.* 2020, 1–15.
- (6) Pill, M. F.; Holz, K.; Preusske, N.; Berger, F.; Clausen-Schaumann, H.; Luning, U.; Beyer, M. K. Mechanochemical Cycloreversion of Cyclobutane Observed at the Single Molecule Level. Chem. Eur. J. 2016, 22 (34), 12034–12039.
- (7) Wang, J.; Kouznetsova, T. B.; Boulatov, R.; Craig, S. L. Mechanical Gating of a Mechanochemical Reaction Cascade. *Nat. Commun.* 2016, 7, 13433.
- (8) Tian, Y.; Cao, X.; Li, X.; Zhang, H.; Sun, C. L.; Xu, Y.; Weng, W.; Zhang, W.; Boulatov, R. A Polymer with Mechanochemically Active Hidden Length. J. Am. Chem. Soc. 2020, 142 (43), 18687–18697.
- (9) Zhang, H.; Li, X.; Lin, Y.; Gao, F.; Tang, Z.; Su, P.; Zhang, W.; Xu, Y.; Weng, W.; Boulatov, R. Multi-Modal Mechanophores Based on Cinnamate Dimers. *Nat. Commun.* 2017, 8 (1), 1147.
- (10) Bowser, B. H.; Craig, S. L. Empowering Mechanochemistry with Multi-Mechanophore Polymer Architectures. *Polym. Chem.* 2018, 9 (26), 3583–3593.
- (11) Zhang, Y.; Wang, Z.; Kouznetsova, T. B.; Sha, Y.; Xu, E.; Shannahan, L.; Fermen-Coker, M.; Lin, Y.; Tang, C.; Craig, S. L. Distal Conformational Locks on Ferrocene Mechanophores Guide Reaction Pathways for Increased Mechanochemical Reactivity. Nat. Chem. 2021, 13, 56–62.
- (12) Rostovtsev, V. V.; Green, L. G.; Fokin, V. V.; Sharpless, K. B. A Stepwise Huisgen Cycloaddition Process: Copper(I)-Catalyzed Regioselective "Ligation" of Azides and Terminal Alkynes. Angew. Chem., Int. Ed. 2002, 41 (14), 2596–2599.
- (13) Malkoch, M.; Vestberg, R.; Gupta, N.; Mespouille, L.; Dubois, P.; Mason, A. F.; Hedrick, J. L.; Liao, Q.; Frank, C. W.; Kingsbury, K.; Hawker, C. J. Synthesis of Well-Defined Hydrogel Networks Using Click Chemistry. *Chem. Commun.* 2006, 2774–2776.
- (14) Zhong, M.; Wang, R.; Kawamoto, K.; Olsen, B. D.; Johnson, J. A. Quantifying the Impact of Molecular Defects on Polymer Network Elasticity. *Science* 2016, 353 (6305), 1264–1268.
- (15) Arora, A.; Lin, T.-S.; Beech, H. K.; Mochigase, H.; Wang, R.; Olsen, B. D. Fracture of Polymer Networks Containing Topological Defects. *Macromolecules* 2020, 53, 7346–7355.

- (16) Akagi, Y.; Gong, J. P.; Chung, U.; Sakai, T. Transition between Phantom and Affine Network Model Observed in Polymer Gels with Controlled Network Structure. *Macromolecules* 2013, 46 (3), 1035–1040.
- (17) Rubinstein, M.; Colby, R. H. Polymer Physics; Oxford University Press: Oxford, U.K., 2003.
- (18) Rivlin, R. S.; Thomas, A. G. Rupture of Rubber. I. Characteristic Energy for Tearing. *J. Polym. Sci.* **1953**, *10* (3), 291–318
- (19) Lee, B.; Niu, Z.; Wang, J.; Slebodnick, C.; Craig, S. L. Relative Mechanical Strengths of Weak Bonds in Sonochemical Polymer Mechanochemistry. J. Am. Chem. Soc. 2015, 137 (33), 10826– 10832.
- (20) Berkowski, K. L.; Potisek, S. L.; Hickenboth, C. R.; Moore, J. S. Ultrasound-Induced Site-Specific Cleavage of Azo-Functionalized Poly(Ethylene Glycol). *Macromolecules* 2005, 38, 8975–8978.
- (21) Smalø, H. S.; Uggerud, E. Ring Opening vs. Direct Bond Scission of the Chain in Polymeric Triazoles under the Influence of an External Force. *Chem. Commun.* 2012, 48 (84), 10443– 10445.
- (22) Lake, G. J.; Thomas, A. G. The Strength of Highly Elastic Materials. Proc. R. Soc. London, Ser. A Math. Phys. Sci. 1967, 300 (1460), 108–119.
- (23) Akagi, Y.; Sakurai, H.; Gong, J. P.; Chung, U. I.; Sakai, T. Fracture Energy of Polymer Gels with Controlled Network Structures. *J. Chem. Phys.* **2013**, *139* (14), 144905.
- (24) Mao, Y.; Talamini, B.; Anand, L. Rupture of Polymers by Chain Scission. *Extrem. Mech. Lett.* **2017**, *13*, 17–24.
- (25) Wang, S.; Panyukov, S.; Rubinstein, M.; Craig, S. L.
 Quantitative Adjustment to the Molecular Energy Parameter in
 the Lake–Thomas Theory of Polymer Fracture Energy.

 Macromolecules 2019, 52, 2772–2777.
- (26) Lin, S.; Zhao, X. Fracture of Polymer Networks with Diverse Topological Defects. *Phys. Rev. E* 2020, 102, 52503.
- (27) Johnson, F. A.; Radon, J. C. Strain Rate-Crack Speed Relation in Steady State Fracture Processes. *Int. J. Fract.* 1974, 10 (1), 125–127.
- (28) Oesterhelt, F.; Rief, M.; Gaub, H. E. Single Molecule Force Spectroscopy by AFM Indicates Helical Structure of Poly(Ethylene Glycol) in Water. New J. Phys. 1999, 1, 6.
- (29) Zhong, M.; Wang, R.; Kawamoto, K.; Olsen, B. D.; Johnson, J. A. Quantifying the Impact of Molecular Defects on Polymer Network Elasticity. *Science* 2016, 353 (6305), 1264–1268.
- (30) Klein, I. M.; Husic, C. C.; Kovács, D. P.; Choquette, N. J.; Robb, M. J. Validation of the CoGEF Method as a Predictive Tool for Polymer Mechanochemistry. J. Am. Chem. Soc. 2020, 142 (38), 16364–16381.
- (31) Kean, Z. S.; Niu, Z.; Hewage, G. B.; Rheingold, A. L.; Craig, S. L. Stress-Responsive Polymers Containing Cyclobutane Core Mechanophores: Reactivity and Mechanistic Insights. *J. Am. Chem. Soc.* 2013, *135* (36), 13598–13604.
- (32) Chen, Z.; Mercer, J. A. M.; Zhu, X.; Romaniuk, J. A. H.; Pfattner, R.; Cegelski, L.; Martinez, T. J.; Burns, N. Z.; Xia, Y. Mechanochemical Unzipping of Insulating Polyladderene to Semiconducting Polyacetylene. Science 2017, 357, 475–479.
- (33) Pauling, L. The Theory of Resonance in Chemistry. *Proc. R. Soc. London, Ser. A Math. Phys. Sci.* 1977, 356, 433–441.
- (34) Ducrot, E.; Chen, Y.; Bulters, M.; Sijbesma, R. P.; Creton, C. Toughening Elastomers with Sacrificial Bonds and Watching Them Break. Science 2014, 344 (6180), 186–189.
- (35) Slootman, J.; Waltz, V.; Yeh, C. J.; Baumann, C.; Göstl, R.; Comtet, J.; Creton, C. Quantifying Rate- and Temperature-Dependent Molecular Damage in Elastomer Fracture. *Phys. Rev.* X 2020, 10 (4), 041045.
- (36) Akbulatov, S.; Tian, Y.; Huang, Z.; Kucharski, T. J.; Yang, Q.-Z.; Boulatov, R. Experimentally Realized Mechanochemistry Distinct from Force-Accelerated Scission of Loaded Bonds. Science 2017, 357, 299–303.
- (37) Pill, M. F.; East, A. L. L.; Marx, D.; Beyer, M. K.; Clausen-Schaumann, H. Mechanical Activation Drastically Accelerates Amide Bond Hydrolysis, Matching Enzyme Activity. *Angew. Chem., Int. Ed.* 2019, 58 (29), 9787–9790.
- (38) Beedle, A. E. M.; Mora, M.; Davis, C. T.; Snijders, A. P.; Stirnemann, G.; Garcia-Manyes, S. Forcing the Reversibility of a Mechanochemical Reaction. *Nat. Commun.* 2018, 9, 3155.

- (39) Huang, W.; Wu, X.; Gao, X.; Yu, Y.; Lei, H.; Zhu, Z.; Shi, Y.; Chen, Y.; Qin, M.; Wang, W.; Cao, Y. Maleimide–Thiol Adducts Stabilized through Stretching. *Nat. Chem.* **2019**, *11*, 310–319.
- (40) Chen, Z.; Zhu, X.; Yang, J.; Mercer, J. A. M.; Burns, N. Z.; Martinez, T. J.; Xia, Y. The Cascade Unzipping of Ladderane Reveals Dynamic Effects in Mechanochemistry. *Nat. Chem.* **2020**, *12*, 302–309.
- (41) Wollenhaupt, M.; Schran, C.; Krupička, M.; Marx, D. Force-

Induced Catastrophes on Energy Landscapes: Mechanochemical Manipulation of Downhill and Uphill Bifurcations Explains the Ring-Opening Selectivity of Cyclopropanes. *ChemPhysChem* **2018**, *19* (7), 837–847.

